Available online at www.sciencedirect.com

ScienceDirect

Energy Procedia 120 (2017) 484–491

Energy Procedia

www.elsevier.com/locate/procedia

INFUB - 11th European Conference on Industrial Furnaces and Boilers, INFUB-11

Burner design for an industrial furnace for thermal post-combustion

Jordan A. Denev[a], Ilian Dinkov[b], Henning Bockhorn[b]*

[a]*Steinbuch Centre for Computing, Karlsruhe Institute of Technology, Kaiserstrasse 12, D-76131 Karlsruhe, Germany*
[b]*Engler-Bunte-Institute, Karlsruhe Institute of Technology, Engler-Bunte-Ring 1-7, D-76131 Karlsruhe, Germany*

Abstract

The industrial furnace considered in this work is designed to remove organic flue gas components by thermal post-combustion. In the existing device air contaminated with organic components is mixed with auxiliary fuel (methane) in a conical diffuser. Optimization of the post-combustion with respect to heat recovery and, thereby, inlet temperatures led to non-proper stabilization of the flame followed by a thermal damage of the conical burner in the existing design. In order to protect the burner from thermal damage, a new robust swirl-induced lifted flame design has been considered. This design includes possibilities of varying the angle of the cone and the swirl number of the incoming mixture. It allows adjusting the lifted flame position as well as improving the oxidation of the organic component while simultaneously lowering the risk of thermal damage of the burner.
The methodology for burner design is based on the numerical simulation of the turbulent reacting flow in the furnace. Results for velocity and temperature fields in the furnace for the old and the new design of the burner are compared. The final, optimized burner design enables the combustion of a wide range of gas mixtures with different calorific values at different thermal loads.

Peer-review under responsibility of the organizing committee of INFUB-11

Keywords: Burner design; furnaces; thermal post-combustiion, numerical simulation

1. Introduction

The industrial furnace considered in this work is designed to remediate organic gaseous compounds evolving with the drying air from drying processes by thermal post-combustion. The contaminated drying air is mixed with auxiliary fuel in a conical burner, which is the main target for optimization in the existing design. Auxiliary fuel is methane.

* Corresponding author. Tel.: +49 (0)721 608 47984; fax: +49 (0)721 608 47770.
E-mail address: henning.bockhorn@kit.edu

1876-6102
Peer-review under responsibility of the organizing committee of INFUB-11
10.1016/j.egypro.2017.07.171

A scheme of the furnace and its main components is given in Fig. 1. The conical burner is responsible for mixing of the air/waste gas mixture with the auxiliary fuel and for stabilization of the flame.

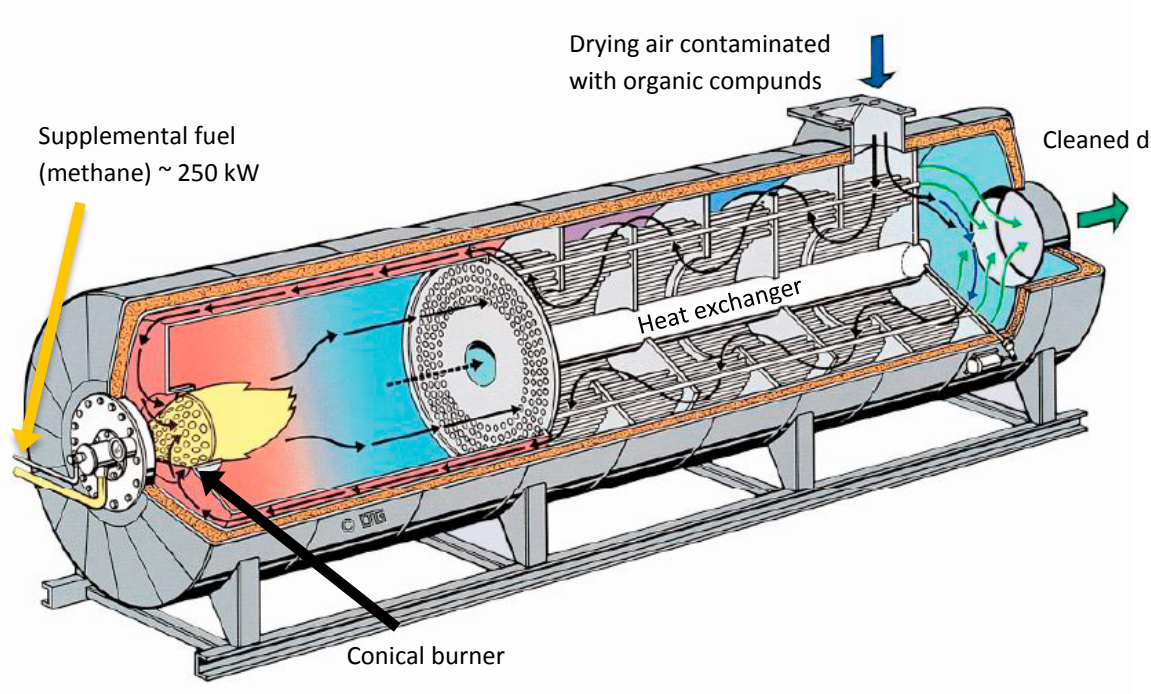

Fig. 1. Scheme of the investigated combustion chamber of the furnace.

The driving force for the work presented in this paper was the thermal damage appearing on the conical burner (thickness 2.5 to 4mm). Initially, the furnace has been operated stable with NO_x emissions below the limits prescribed in Europe, see e.g. [1]. To improve the thermal efficiency of the drying process, a shell-and-tube heat exchanger has been included as a part of the original equipment. It allowed fuel savings up to 50% on an annual basis. After modification the temperature of the contaminated drying air increased from approx. 410 [^{o}C] to approx. 550 [^{o}C] when leaving the heat exchanger and entering the ring gap of the furnace, see Fig. 1. This led to a strong permanent deformation causing a thermal damage of the conical burner. Consequently, the flame stabilisation mechanism was deteriorated and the NO_x emissions were rising above the limits of the legal constraints.

The objective of this work was the design of a completely new conical burner that overcomes the problem of thermal damage. This design includes possibilities of varying the angle of the cone and the swirl strength of the air/waste gas mixture. It allows adjusting the lifted flame position and decreasing the temperature of the burner.

The methodology of the work is based on the use of numerical simulation of the turbulent reacting flow in the furnace. For this purpose, the operating parameters of the furnace were analyzed first. The analysis included the identification of the waste gas contents and composition and its influence on the combustion in the furnace. Second, a chemical reaction scheme was developed including combustion of the waste gas components. After implementation of this reaction scheme into a commercially available Computational Fluid Dynamics (CFD) tool, the furnace has been simulated for different operating conditions. Finally, the CFD tool was used to develop and optimize the geometric parameters of the newly designed burner.

2. Analysis of the combustion parameters of the furnace

During the drying process of varnished metal parts, the drying air absorbs the volatile components of the solvents used for the dyes in the preceding varnishing operations. An analysis of these solvents showed benzene and partly naphthalene being predominant components of the solvents. Therefore, the influence of benzene and naphthalene on

the combustion properties of air/waste gas mixtures in dependence on inlet temperature is important. Typical cases studied are given in Table 1.

Table 1. Simulated combustion mixtures for the present analysis.

Case	Species	Description
1	Methane	Reference case: stoichiometric composition
2	Methane and benzene	Methane (20 m^3/h) and air (10000 m^3/h) containing benzene (8,6 g/m^3)
3	Methane and naphthalene	Methane (20 m^3/h) and air (10000 m^3/h) containing naphthalene (8,6 g/m^3)
4	Methane and benzene, naphthalene	Methane (20 m^3/h) and air (10000 m^3/h) containing benzene and naphthalene (equal mole fractions with a total amount of 8,6 g/m^3)

For the general analysis of the combustion properties, the detailed chemical reaction mechanism of [2] was employed. First, the adiabatic flame temperatures were studied for three different initial temperatures of the air/waste gas mixture. The first temperature, 700 [K], corresponding to the conditions before the modification of the heat exchanger, the second, 823 [K], corresponding to the conditions after the modification and the third one, 900 [K], corresponding to the conditions at the burner inlet after preheating the air with the flue gases in the ring gap. For all three initial temperatures, the applied contents of benzene and naphthalene increase the adiabatic combustion temperatures up to 30 [K] above the reference case.

In a second step, the ignition delay times of the cases from Table 1 have been compared. The ignition delay times are calculated from the time change of the OH-radical concentrations computed with the software HOMREA [3]. The simulations were carried out for a homogeneous reactor with 1 m^3 volume at 1 bar pressure. The calculated ignition delay times demonstrate that benzene has the strongest influence on the ignition delay times. With increasing temperature, benzene reduces the ignition delay time by almost one order of magnitude compared to the reference case with pure methane. The smaller ignition delay time may shorten the distance between the flame and the burner surface and, therefore, lead to higher thermal loads on the burner. The lower autoignition temperature of benzene (T_{ai_b} = 498 [°C]) compared to that of naphthalene (T_{ai_n} = 525 [°C]) and the shorter ignition delay times increase the possibility for pre-combustion reactions even in the ring gap after the heat exchanger. This also leads to higher thermal loads of the burner when more benzene is present in the air/waste gas mixture. Therefore, benzene is regarded as the most unfavourable case for decreasing the risk of thermal damage of the burner. Consequently, benzene as the constituent of the waste gas (case 2 from Table 1) was chosen the further investigation.

3. Description of the CFD method and boundary conditions

For the performed CFD calculations a commercial code (ANSYS CFX12) was employed utilizing the existing discretization methods and detailed thermochemical and transport data basis. The Finite Rate Chemistry formulation is used to calculate the heat release of the methane/benzene oxidation. This formulation computes the chemical source terms (rate of species consumption/production) using rate expressions as given in Eq. (1) and an Arrhenius temperature dependence of the rate coefficients. The chemical rate expression gives the rate R_k of reaction k as

$$R_k = F_k \prod_{I=A,B,\ldots}^{N_C} c_I^{\,r_{kI}} = A_k T_g^{\beta_k} \exp\left(-\frac{E_k}{RT_g}\right) \cdot \prod_{I=A,B,\ldots}^{N_C} c_I^{\,r_{kI}} \tag{1}$$

where c_I is the molar concentration of component I and F_k are the rate coefficients. r_{kI} represents the reaction order of

component I in the reaction k. Here A_k is the pre-exponential factor, β_k is the temperature exponent (dimensionless), E_k is the activation energy *[J/mol]*, T_g is the absolute gas temperature *[K]* and R is the ideal gas constant *[J/(mol.K)]*.

With the reaction rate R_k the source term S_I in the balance equations for the chemical species is given by

$$S_I = W_I \sum_{k=1}^{K} \left(-\upsilon_{kI}\right) R_k \tag{2}$$

where W_I is the molecular weight and ν_{kI} are the stoichiometric coefficients. Here K is the total number of reactions where species I is involved in. With this the Favre-averaged balance equations for species I become

$$\frac{\partial \overline{\rho}\, \tilde{w}_i}{\partial t} = -\frac{\partial \overline{\rho}\, \tilde{u}_j\, \tilde{w}_i}{\partial x_j} + \frac{\partial}{\partial x_j}\left(\frac{\mu_t}{Sc_t} \frac{\partial \tilde{w}_i}{\partial x_j} \right) + \overline{S_i} \tag{3}$$

where w_i are the mass fractions of the chemical species. Description of the reaction scheme and the calculation of the rate coefficients are presented in section 4. In addition to mass balances for the chemical species, the balance equations for total mass, momentum and energy are solved [4].

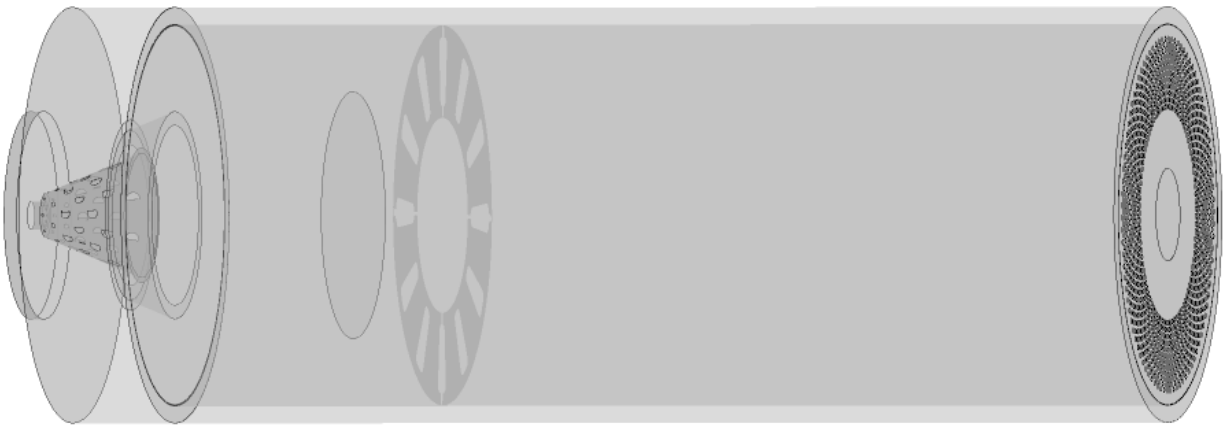

Fig. 2. Scheme of the computational domain.

Table 2. Inflow boundary conditions used for the calculations.

Component	Flow rate	Inlet temperature
Air	10000 [m^3/h]	410 [°C]/550 [°C] (old/new heat exchanger)
Methane (CH_4)	26 [m^3/h]	25 [°C]
Benzene (C_6H_6)	8,6 [g/m^3]	410 [°C]/550 [°C] (old/new heat exchanger)

The computational domain for the calculations, see Fig. 2, comprises the whole furnace, including the conical burner, air/waste gas inflow channel (ring gap in Fig. 1), ending at the entry of the heat exchanger. Additionally, the heat transfer between the furnace and the air/waste gas inflow channel is also considered in the numerical calculations. The resulting numerical grid was locally refined near the walls and the burner region. It comprised approx. 10 Mio. elements (3 Mio. nodes).

The used CFD-code employs the finite volume method of a cell-centered storage arrangement. The applied discretization for the momentum equations is based on a bounded linear scheme. For considering heat radiation, the discrete transfer radiation (weighted sum of gray gases) model is used with mixture averaged properties of the gas phase. The numerical calculations were carried out using the inflow boundary conditions summarized in Table 2. The furnace is regarded as adiabatically insulated to the ambient. For turbulence modelling the k-ε-model as implemented in CFX 12 has been used [4].

4. Reduction of a detailed chemical kinetic model for the use in the present computational fluid dynamics (CFD) simulations

Detailed chemical kinetic models for hydrocarbon fuels contain a large number of species and elementary reactions – typically in the order of several hundreds. Due to their high computational cost these detailed models are not directly applicable for use in three-dimensional CFD-simulations, especially when targeting industrial applications. Instead of using detailed chemical kinetic mechanisms, the usual practice is to employ reduced or global mechanisms, which contain only the most important species.

While many reduced/global models for use in CFD-simulations exist, see e.g. [5], the engineering practice often requires assembling new combinations of fuels and operating conditions. In these cases, new global reaction mechanisms with few chemical species and few reactions have to be designed. One possible methodology consists of the following 5 steps:

Step 1: Choosing a detailed reaction mechanism containing the educts and products for the applied combination of fuels. In the present study the considered fuels consist of mixtures of methane and benzene and the oxidizer is air. The detailed reaction mechanism of Appel et al. [2] consisting of 538 reactions between 101 species is applied.

Step 2: Selecting the number of species and global reactions for use in the final model to be implemented into the CFD-code. In the present case balance equations for the six chemical species C_6H_6, CH_4, O_2, CO, H_2O and CO_2 have been applied. They were combined using a reaction scheme defined by 3 global reactions:

$$CH_4 + 3/2O_2 \rightarrow CO + 2H_2O \quad \text{(R1)}$$
$$C_6H_6 + 9/2\ O_2 \rightarrow 6CO + 3H_2O \quad \text{(R2)}$$
$$CO + 1/2\ O_2 \rightarrow CO_2 \quad \text{(R3)}$$

Step 3: Identifying the range of concentrations of main species and temperatures for the targeted combustion process. Performing a number of time dependent PSR-calculations and recording the traces for the main species. In the performed calculations, the amount of benzene is varied according to the needs of the industrial process and an appropriate amount of methane is added to obtain the right temperature in the combustion chamber which would lead to low pollutant emissions in the exhaust gases.

The number of parameter combinations used for the present investigation was 108. Therefore, 108 time dependent PSR-calculations have been carried out using the software HOMREA [3]. The transient intermediates are recorded and in total more than 38000 state points for the main variables are obtained. This database has to be fitted to the global reaction mechanism to obtain the rate coefficients and the rate-of-production terms for the main species.

Step 4: Performing a best fit to the rate-of-production terms using genetic algorithms (GA). The parameters that need to be fitted are those from the Arrhenius form of the rate-of-production terms from Eq. (1). The 10 coefficients for the first and second reaction are fitted with a genetic algorithm. The coefficients for the third reaction are taken from [5].The results from this fit are listed in Table 3 (dimensions are in *cm-sec-mole-kcal-Kelvin*).

The software for the genetic algorithm is an add-in solver for Excel [6]. The initial population contains 300 individuals, the crossover probability is 0.3 and the mutation probability is 0.45. The fitness of the individuals is assessed separately for each fuel in terms of the sum of squared deviations from the original rate-of-production values.

Step 5: Implementing the global model in the CFD-program to obtain the source-terms in the balance equations for the main species. In this step the results listed in Table 3 are implemented in the ANSYS-CFX software (by means of the CCL-interface language) which is then used for the simulation of the flow, temperature and species distribution in the combustion chamber. Averaging of the source term was achieved by weighting the reaction rates from Eq. (2) with a temperature-β-function-pdf.

Table 3. Results for the parameters from the applied genetic algorithm.

k	A_k	β_k	E_k	$r_{k,\,Fuel}$	$r_{k,\,Ox}$
1	4,73E+13	-1,17	51,09	0,44	0,51
2	6,41E+13	-0,91	50,23	0,51	0,77
3	3,98E+14	0,00	40,00	1,00	0,25

5. Numerical Results

Figures 3 and 4, left, present the local axial velocity and temperature from the numerical simulations along the middle plane of the furnace that is parallel to the main flow direction in the furnace. The calculations are obtained with an air/waste gas mixture preheating temperature of 410°C, which is the case for the unmodified heat exchanger.

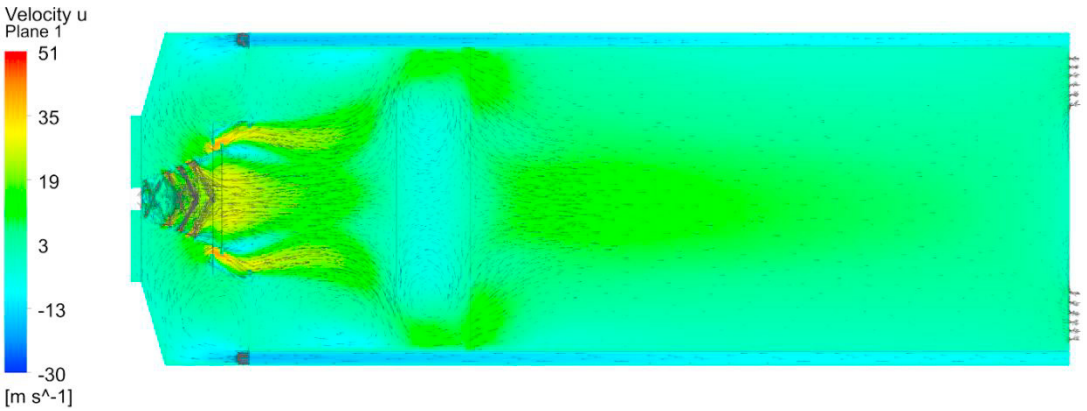

Fig. 3. Local axial velocity distribution along the middle plane of the furnace.

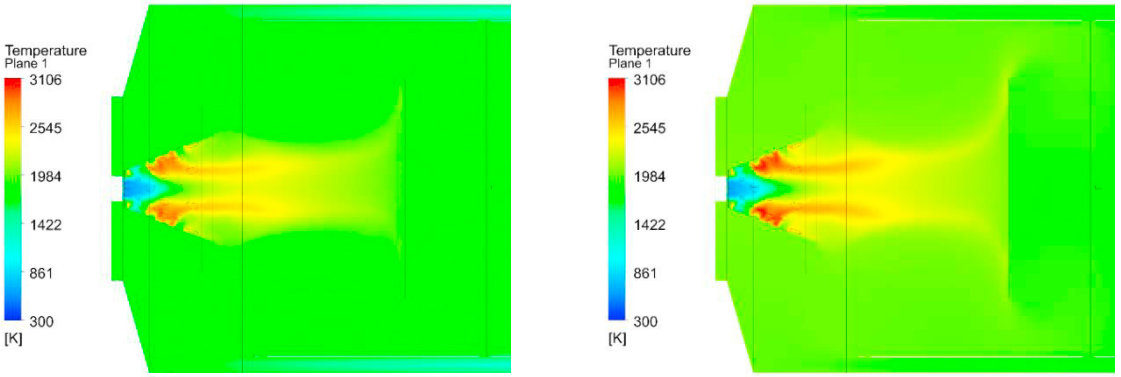

Fig. 4. Temperature distribution along the middle plane of the furnace; left: unmodified heat exchanger; right: modified heat exchanger.

The incoming air/benzene flow is accelerated after entering the ring gap of the furnace and is preheated along the wall between the main combustion chamber and the ring gap. After being deflected at the end of the ring gap, the air/benzene flow enters the conical burner, is mixed with methane and the combustion takes place. Figure 4, left, displays the high temperature region near the conical burner. The maximum gas temperature in this case is 2937 [K].

Comparing operating conditions of the unmodified heat exchanger with that of the modified one in Fig. 5 the increased temperature of the incoming air/waste gas mixture leads also to higher burner surface temperatures. These temperatures are approx. 169 [K] higher compared with the case with the unmodified heat exchanger. This increase leads to a thermal damage of the burner manifested by a strong deformation. The thermal damage occurs exactly at the location of the highest temperatures. The modification of the heat exchanger increased the thermal efficiency of the drying process, however, it led to a higher surface temperature of the burner and to its thermal damage.

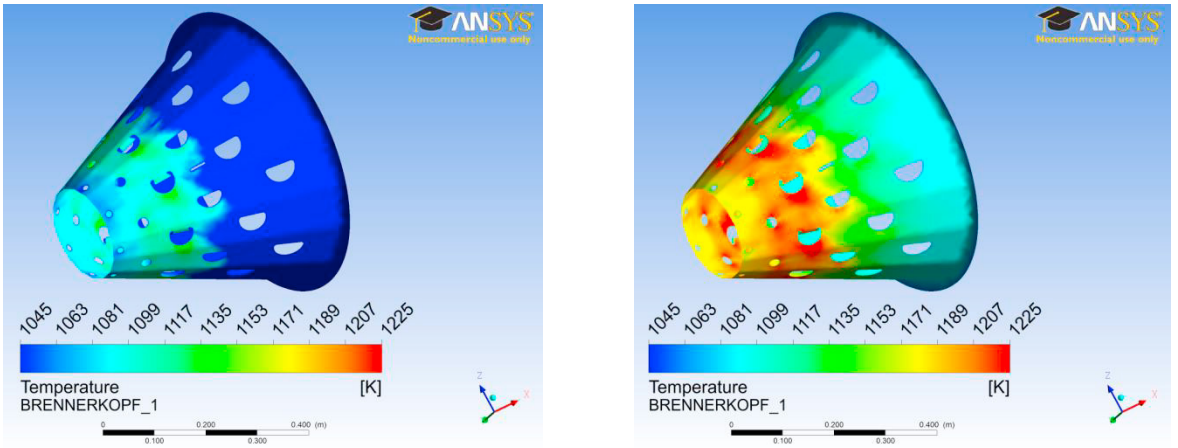

Fig. 5. Temperature of the steel mantle of the burner before modification of the heat exchanger, inlet temperature 410 [°C] (left) and after improving the heat exchanger, inlet temperature 550 [°C] (right), see Table 2 for inlet conditions.

The aim of the present work was to escape from this disadvantage by designing a new robust burner, which allows adjusting the flame in a lifted position and preventing the burner material from thermal damages. For that, a design has been developed allowing control of the flame shape by applying high swirl [7] with high tangential velocity. To achieve this, the burner shape was changed: instead of having a large amount of small inlet openings for the air/benzene mixture, the burner was equipped with adjustable vents. The geometry of the vents and the conical angle have been optimized. The target of the optimization was to stabilize the flame downstream in a lifted position while simultaneously keeping the pressure drop low for a wide range of operating conditions.

This newly developed design is depicted in Fig. 6, left. The shape of the burner includes possibilities to use varying cone angles. This allows controlling the size of the effective inflow area, thus adjusting the swirl strength of the flow. Consequently, this stabilization method results in a lifted flame position that is adjustable downstream of the burner. Figure 6, right, clarifies further the typical behaviour of a swirled flow with a negative velocity at the symmetry axis of the burner. Figure 7, left, demonstrates the downstream stabilisation of the flame leading to an efficient protection against variation of thermal loads and preventing thermal damage. The temperature distribution of the new burner design (with considerably lower temperatures of the burner surface is depicted in Fig. 7, right.

Conclusions

In the present work a new robust burner design for a post-combustion facility has been developed. The methodology is based on the use of numerical simulation of the turbulent reacting flow in the furnace using a commercial CFD-code as a major design tool. For the efficient application of the CFD-tools some preparatory modelling steps had to be performed comprising the development and adaptation of reduced chemical kinetics for the range of operating conditions as well as the implementation of the model into the commercial CFD-simulation tool.

In order to protect the burner from thermal damage at the given operating conditions, a new swirl-induced lifted flame design has been developed. It allows adjusting the lifted flame position in downstream direction which decreases the temperature of the burner sheet.

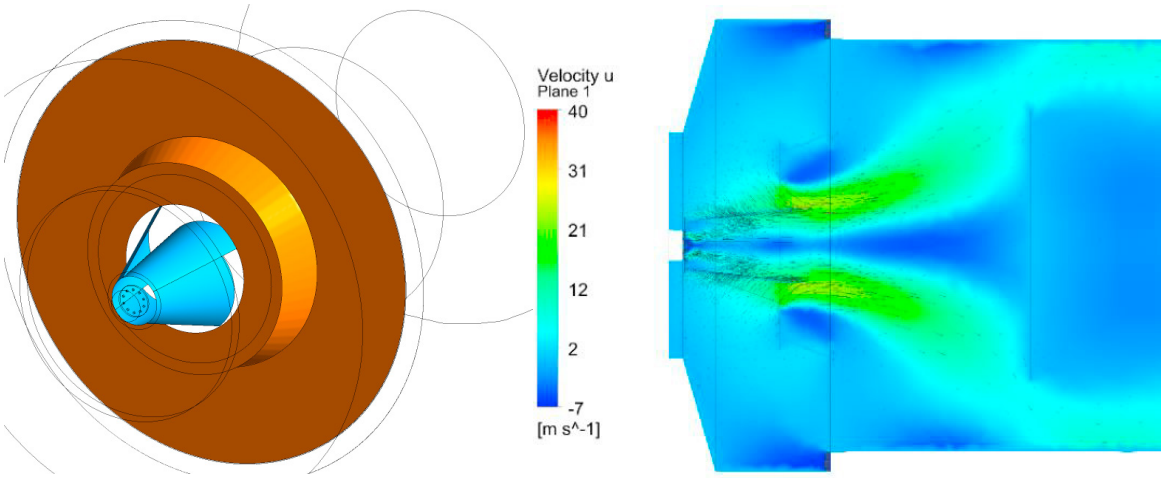

Fig. 6. Geometry of the new burner and local axial velocity distribution along the middle plane of the furnace.

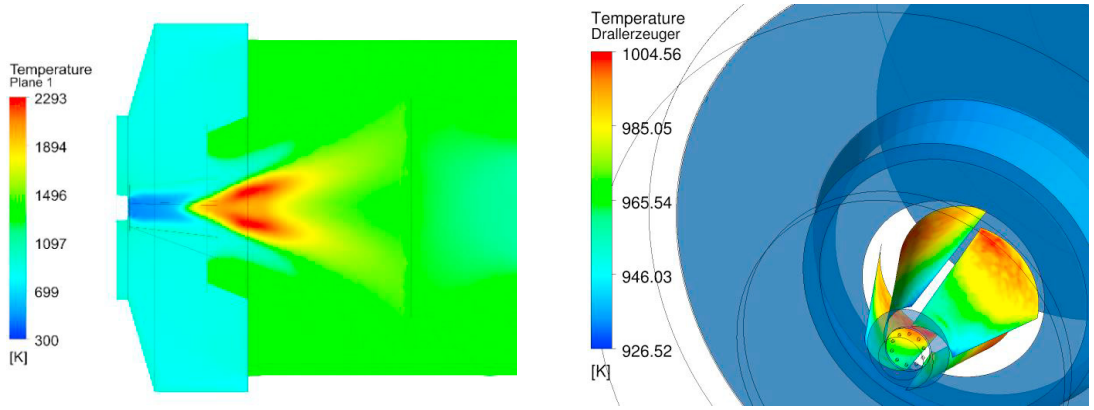

Fig. 7. Local temperature along the middle plane of the furnace and temperature of the burner surface of the new burner design.

References

[1] Directive (EU) 2015/2193 of the European Parliament and of the Council of 25 November 2015 on the limitation of emissions of certain pollutants into the air from medium combustion plants.

[2] Appel, J., Bockhorn, H. and Frenklach, M. Kinetic Modeling of Soot Formation with Detailed Chemistry and Physics: Laminar Premixed Flames of C2 Hydrocarbons, Combust. Flame 121 (2000) pp.122-136 .

[3] Software package HOMREA. Institute of Technical Thermodynamics, KIT. (http://www.itt.kit.edu/english/827.php) .

[4] ANSYS, 2010.ANSYS CFX 12 User's Manuals.

[5] Westbrook, C.K. and F.L. Dryer, F.L. Simplified Reaction Mechanisms for the Oxidation of Hydrocarbon Fuels in Flames, Combustion Science and Technology 27 (1981) pp.31-43.

[6] Software GeneticSolver for Excel. Noyan Turkkan, Université de Moncton, Canada .

[7] Denev, J.A., J. Fröhlich, J. and H. Bockhorn, H. Large eddy simulation of a swirling transverse jet into a crossflow with investigation of scalar transport, Phys. Fluids 21(1), 015101 (2009), 20 pages; DOI:10.1063/1.3054148 .